

ON VERTICAL ANALYSIS OF RAILWAY TRACK VIBRATIONS

Traian MAZILU¹, Mădălina DUMITRIU¹, Cristina TUDORACHE¹, Mircea SEBEȘAN²

¹University “Politehnica” of Bucharest, Department of Railway Vehicles, Romania

²METROREX, Bucharest, Romania

E-mail: trmazilu@yahoo.com

The paper herein presents a vertical vibration analysis of the ballasted track using a new model of the periodic support of the rail that improves the prediction of the rail response for both low and high frequencies. The model of the periodic support consists of two three-directional Kelvin-Voigt systems for the rail pad and the ballast, and a mixed Kelvin-Voigt/Maxwell system for the subgrade. Also, the inertia of the sleeper and the ballast block are introduced. The rail response due to a stationary and moving harmonic load is analyzed by applying the Green’s functions method. The influence of the rail pad stiffness and of the Doppler effect on railkway track vibrations are presented.

Key words: Rail; Timoshenko beam; Periodic support; Green’s functions; Doppler effect.

1. INTRODUCTION

The study of the vertical vibration of the ballasted track is critical when analysing the wheel/rail interaction in order to give practical solutions for certain issues such as formation of wheel and rail corrugation [1], generation of rolling noise [2] or track damage.

Usually, the track model is reduced to a rail resting on discrete supports including the elastic rail pads, the inertia of the sleepers and the elasticity of the ballast [3]. However, even if the Timoshenko beam model is used for the rail with a greater accuracy than the Euler-Bernoulli beam model – as the shear and the rotary inertia of the cross-section are taken into account – two frequencies ranges still remain critical. On the one hand, the rail receptance is underestimated at low frequencies (bellow 50 Hz). On the other hand, for the frequencies that are situated within the ‘pinned-pinned’ frequency range, the rail receptance at mid span is over-estimated.

To obtain a good agreement between the prediction and the experimental results, Zhai et al. [4] and Nielsen [5] have introduced the inertia of the ballast and the elasticity of the subgrade. Despite of these improvements, it seems that the subgrade models proposed (a single Kelvin-Voigt system [4] or two Kelvin-Voigt systems connected in series [5]) are not as appropriate as to simulate the rail response at low frequencies. It has to be emphasized that Knothe and Wu [6] have obtained an increase of the rail receptance when the frequency decreases bellow 50 Hz, according to the measurements, upon using a sophisticated ballast-subgrade model starting from the theory of the elastic half-space. However, the time-domain analysis of the wheel/rail interaction requires a simpler solution for the track model.

In regards to the prediction of the rail response at the pinned-pinned resonance, the realistic results are obtained when the limitation of the rail cross-section rotation by the rail pad is considered, and the three-directional rail pad model is used [7].

The dynamic response of the periodic structures under moving forces has been extensively analyzed in the past 30 years and different methods have been proposed. Floquet theorem was applied by Krzyzynski and Popp [8], and Krzyzynski [9], the Fourier-series approach has been used by Sheng et al. [10], while Nordborg [11] has developed the Green’s functions method.

The paper herein presents an analysis of the vertical vibration of the ballasted track, considering a new model for the rail support that gives a good agreement between the prediction and the measurements. The Green’s functions method, previously proposed by the present author [12, 13], is applied to point out the response of the rail under a stationary and moving harmonic force. Also, the influence of the rail pad stiffness and the load velocity (the Doppler effect) are presented.

2. MECHANICAL MODEL

One presumes that the track is a symmetric structure and the two rails vibrate independently due to the elasticity of the sleepers. In such circumstances, the track model is reduced to an infinite Timoshenko beam (the rail) resting on discrete pads, each of them including the rail pad, semi-sleeper, ballast block and subgrade (Fig. 2.1). A moving force $P(t)$ travels along the rail head with constant speed V ; t stands for time.

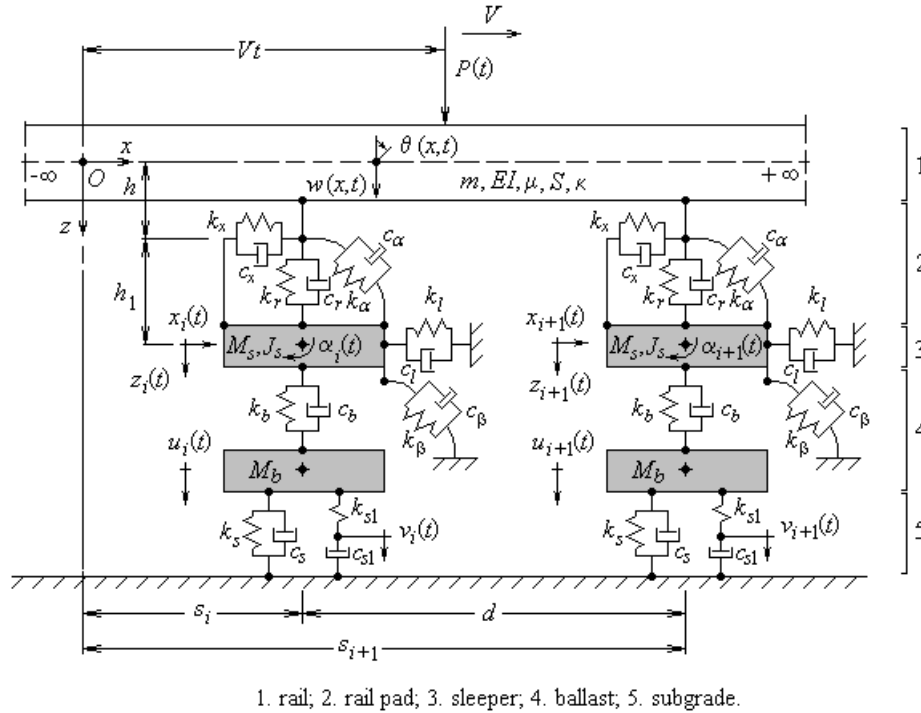


Fig. 2.1.

The motion of the rail is described by the column vector $\{\mathbf{q}\} = [w(x,t) \theta(x,t)]^T$, where $w(x,t)$ and $\theta(x,t)$ stand for the vertical displacement, respectively the rotation of the cross-section; x is the coordinate along the rail. The parameters for the rail are as follows: the mass per length unit m , the cross-sectional area S , the area moment of inertia I , the density ρ , the Young's modulus E , the shear modulus μ and the shear coefficient κ , the distance between the cross-section's neutral fibre and the rail foot h .

The rail pad is taken as a three-directional Kelvin-Voigt system working in the longitudinal and vertical directions and the rotation in the vertical plane of the rail. The elastic constants k_x , k_z and k_α and the damping constants c_x , c_z and c_α are related to the rail pad.

The semi-sleepers are equidistant by the sleeper bay of the d length; the semi-sleeper i is placed at the s_i distance from the reference frame. It is assumed that the semi-sleeper is a rigid body having three-degree of freedom: the vertical $z_i(t)$ and longitudinal $x_i(t)$ translations and the rotation $\alpha_i(t)$ in the vertical plane. Each semi-sleeper has the mass M_s and the mass-moment of inertia J_s . The distance between the semi-sleeper centroid and the rail pad is h_1 .

The ballast influence is simulated by inserting a set of separate masses under semi-sleepers via Kelvin-Voigt systems. In addition, the longitudinal and rotational resistance of the ballast are modelled using two Kelvin-Voigt systems.

Assuming that the load velocity is much lower than the velocity of the waves excited in subgrade by the moving load, it can reduce the subgrade model under one supporting point to a mixed Kelvin-Voigt/Maxwell system. The proposed solution is different from the familiar ones given by Zhai et al. [4] or Nielsen [5] and it is advantageous due to the good agreement between the prediction and measurements within the low frequencies. The parameters for the ballast and the subgrade are as follows: the vibrating mass of ballast M_b , the elastic constants k_u , k_b , k_s and k_{s1} and the corresponding damping constants c_u , c_b , c_s and c_{s1} .

The displacement of the ballast block under the sleeper i is $u_i(t)$, while $v_i(t)$ is the displacement from the subgrade model. All displacements of the support model are contained in the column vector $\{\mathbf{q}_i^s\} = [x_i(t) z_i(t) \alpha_i(t) u_i(t) v_i(t)]^T$.

The track's differential equations of motion may be formulated in the matrix form as

$$\mathbf{T}_{x,t} \{\mathbf{q}\} - \sum_{i=-\infty}^{\infty} (\mathbf{A}_i \{\mathbf{q}_i\} - \mathbf{B}_i \{\mathbf{q}_i^s\}) \delta(x - s_i) = \{\mathbf{P}\}, \quad (2.1)$$

$$\mathbf{C}_i \{\mathbf{q}_i^s\} = \mathbf{B}_i^T \{\mathbf{q}_i\}$$

where $\{\mathbf{P}\} = [-P(t)\delta(x-Vt) \ 0]^T$ is the column vector of the forces on the rail and $\delta(\cdot)$ is the Dirac's delta function, $\mathbf{T}_{x,t}$ stands for the Timoshenko's matrix operator and $\mathbf{A}_i, \mathbf{B}_i, \mathbf{C}_i$ are the matrix differentials

$$\mathbf{T}_{x,t} = \begin{bmatrix} \kappa\mu S \frac{\partial^2}{\partial x^2} - m \frac{\partial^2}{\partial t^2} & -\kappa\mu S \frac{\partial}{\partial x} \\ \kappa\mu S \frac{\partial}{\partial x} & EI \frac{\partial^2}{\partial x^2} - \kappa\mu S - \rho I \frac{\partial^2}{\partial t^2} \end{bmatrix}, \mathbf{A}_i = \begin{bmatrix} c_r \frac{d}{dt} + k_r & 0 \\ 0 & c_\theta \frac{d}{dt} + k_\theta \end{bmatrix}$$

$$\mathbf{B}_i = \begin{bmatrix} 0 & c_r \frac{d}{dt} + k_r & 0 & 0 & 0 \\ -h \left(c_x \frac{d}{dt} + k_x \right) & 0 & \Delta c_\alpha \frac{d}{dt} + \Delta k_\alpha & 0 & 0 \end{bmatrix}, \quad (2.3)$$

$$\mathbf{C}_i = \begin{bmatrix} D_x & 0 & h_1 \left(c_x \frac{d}{dt} + k_x \right) & 0 & 0 \\ 0 & D_z & 0 & -c_b \frac{d}{dt} - k_b & 0 \\ h_1 \left(c_x \frac{d}{dt} + k_x \right) & 0 & D_\alpha & 0 & 0 \\ 0 & -c_b \frac{d}{dt} - k_b & 0 & D_u & -k_{s1} \\ 0 & 0 & 0 & -k_{s1} & D_v \end{bmatrix}$$

with

$$D_x = M_s \frac{d^2}{dt^2} + (c_x + c_l) \frac{d}{dt} + k_x + k_l, D_z = M_s \frac{d^2}{dt^2} + (c_r + c_b) \frac{d}{dt} + k_r + k_b, D_v = c_{s1} \frac{\partial}{\partial t} + k_{s1},$$

$$D_\alpha = J_s \frac{d^2}{dt^2} + (c_\alpha + c_\beta + h_1^2 c_x) \frac{d}{dt} + k_\alpha + k_\beta + h_1^2 k_x, D_u = M_b \frac{d^2}{dt^2} + (c_b + c_s) \frac{d}{dt} + k_b + k_s + k_{s1}, \quad (2.4)$$

$$c_\theta = c_\alpha + h^2 c_x, k_\theta = k_\alpha + h^2 k_x, \Delta c_\alpha = c_\alpha - h h_1 c_x, \Delta k_\alpha = k_\alpha - h h_1 k_x.$$

All initial conditions are null and the boundary conditions are null as well

$$\{\mathbf{q}(x,t)\} = [0 \ 0]^T, \{\mathbf{q}_i^s(t)\} = [0 \ 0 \ 0 \ 0 \ 0]^T,$$

$$\lim_{|x-Vt| \rightarrow \infty} \{\mathbf{q}(x,t)\} = [0 \ 0]^T, \lim_{i \rightarrow \pm\infty} \{\mathbf{q}_i^s(t)\} = [0 \ 0 \ 0 \ 0 \ 0]^T. \quad (2.5)$$

The solution of the problem can be formulated using the Green's functions method [12, 13]. According to the convolution theorem and taking into account the causality condition of the track model, the solution of the problem may be given as

$$\begin{aligned} \{q(x, t)\} &= \int_{-\infty}^{\infty} \int_0^t \{g(x, \xi, t - \tau)\} P(\tau) \delta(\xi - V\tau) d\tau d\xi = \int_0^t \{g(x, V\tau, t - \tau)\} P(\tau) d\tau, \\ \{q_i^s(t)\} &= \int_{-\infty}^{\infty} \int_0^t \{g_i^s(\xi, t - \tau)\} P(\tau) \delta(\xi - V\tau) d\tau d\xi = \int_0^t \{g_i^s(V\tau, t - \tau)\} P(\tau) d\tau. \end{aligned} \quad (2.6)$$

where the column vectors

$$\begin{aligned} \{g(x, \xi, t - \tau)\} &= [g^w(x, \xi, t - \tau) \quad g^{\theta}(x, \xi, t - \tau)]^T, \\ \{g_i^s(\xi, t - \tau)\} &= [g_i^x(\xi, t - \tau) \quad g_i^z(\xi, t - \tau) \quad g_i^{\alpha}(\xi, t - \tau) \quad g_i^u(\xi, t - \tau) \quad g_i^v(\xi, t - \tau)]^T \end{aligned} \quad (2.7)$$

contain the Green's functions of the track for the time-domain analysis, which gives the response of the rail in the x section and, respectively the response of the support i at $t - \tau$ moment, due to an unit impulse force applied at the τ moment in rail section ξ .

The displacement of the rail at the loading point is of particular interest from the perspective of the track response. This displacement results from equation (2.6) setting $x = Vt$

$$w(Vt, t) = \int_0^t \{g^w(Vt, V\tau, t - \tau)\} Q(\tau) d\tau, \quad (2.8)$$

where the function $g^w(Vt, V\tau, t - \tau)$ represents the time-domain Green's function of the rail at the loading point. The time-domain Green's function $g^w(Vt, V\tau, t - \tau)$ gives the response of the rail in the Vt moving section at $t - \tau$ moment due to a moving unit impulse force placed in the section $V\tau$ at the moment τ .

Considering a certain time partition, the function $g^w(Vt, V\tau, t - \tau)$ along a sleeper bay can be organized as a matrix – *the Green's matrix of the track*. Finally, the rail displacement at the loading point is calculated numerically using the properties of the Green's functions of the rail to be periodic and attenuated.

Setting $t^* = t - \tau$, the section $x = Vt$ is fixed and we have the function $g^w(x = Vt, Vt - Vt^*, t^*)$ that describes the rail response at the t^* moment due to a moving unit impulse, which starts from the fixed section $x = Vt$ at the initial moment and travels from the right to the left at the velocity of V . Actually, this function is the time-domain Green's function of the rail under moving unit impulse load. Performing the Fourier transform with respect to t^* , the rail receptance for the moving harmonic force results. In this way, the amplitude of the rail, taken as a complex value, is obtained for the particular case only when a moving unit harmonic force passes over the fixed section of the rail.

3. NUMERICAL APPLICATION

In this section, numerical results from a particular ballasted track model under a moving harmonic load are produced using the presented approach showcased. The case of the stationary harmonic load is taken as the reference case.

The parameters for the rail are: $m = 60$ kg/m, $S = 7.69 \cdot 10^{-3}$ m², $I = 30.55 \cdot 10^{-6}$ m⁴, $h_0 = 0.08$ m, $\rho = 7,850$ kg/m³, $E = 210$ GPa, $\mu = 81$ GPa and $\kappa = 0.4$.

The parameters for the discrete support are chosen as: $M_s = 145$ kg, $J_s = 1.28$ kgm², $M_b = 2,500$ kg, $d = 0.6$ m, $h_1 = 0.116$ m, $k_x = 50$ MN/m, $k_r = 280$ MN/m, $k_{\alpha} = k_r c^2 / 3 = 597$ kNm/rad ($2c = 160$ mm, rail pad width), $k_u = 39.6$ MN/m, $k_b = 120$ MN/m, $k_s = 60$ MN/m, $k_{s1} = 100$ MN/m, $c_x = 10$ kNs/m, $c_r = 30$ kNs/m, $c_{\alpha} = c_r c^2 / 3 = 64$ Nms/rad, $c_u = 52$ kNs/m, $c_b = 70$ kNs/m, $c_s = 150$ kNs/m and $c_{s1} = 600$ kNs/m.

For the numerical simulation, the track model length is of 50 sleeper bays; this length satisfies the mandatory demand to preserve the periodic feature of the track in the central zone of the model. Only the rail receptance from this zone is utilized in order to calculate the Green's matrix of the track.

Figure 3.1 shows the receptance of the rail at loading point due to the stationary harmonic excitation for both excitation acting at mid span and above a sleeper in the domain of 0 – 1,600 Hz. One can observe that the rail receptance increases below 50 Hz, due to the influence of the ballast and the subgrade. This aspect is consistent with the results derived from the measurements presented by Knothe and Wu [6].

Within the range of the mid frequencies, the rail and the sleepers vibrate like a system with two-degree of freedom and, because of this, the rail receptance is dominated by two resonance frequencies (about 120

and 480 Hz). The sleepers play the role of a vibration absorber, which explains why the rail has an anti-resonance frequency at circa 240 Hz, between the two resonances. At lower frequencies, the rail and the sleeper are in phase and then, beyond the anti-resonance frequency, they vibrate in anti-phase.

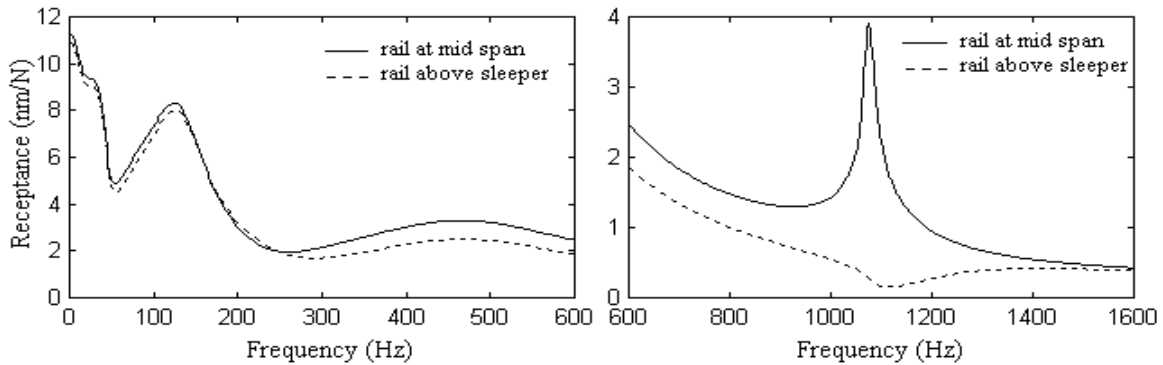


Fig. 3.1.

As we can see, the effect of the periodic support of the rail becomes more evident when the frequency is higher than the anti-resonance frequency and the rail vibrates more intensely at mid span than above sleeper. The highest difference appears at the pinned-pinned resonance frequency, respectively at 1 074 Hz, when the bending wavelength equals twice the span. Also, one has to observe the anti-resonance zone located at 1 120 Hz when the harmonic load is applied above the sleeper.

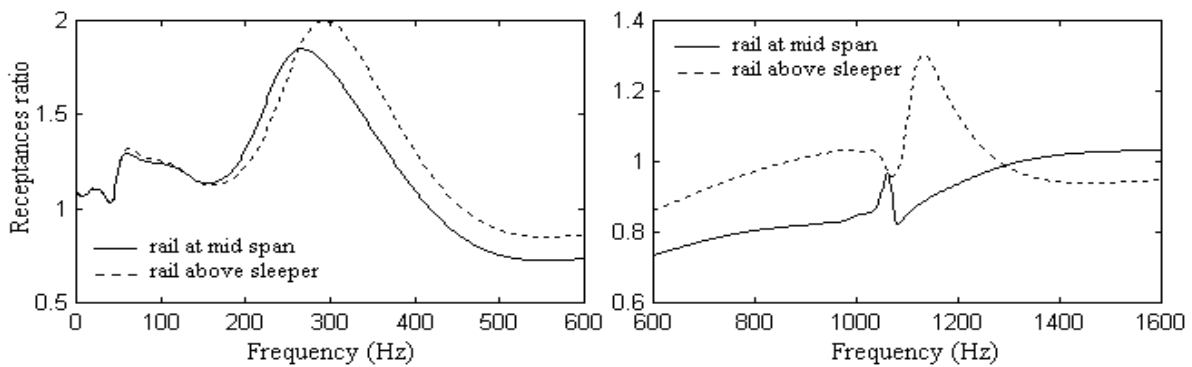


Fig. 3.2.

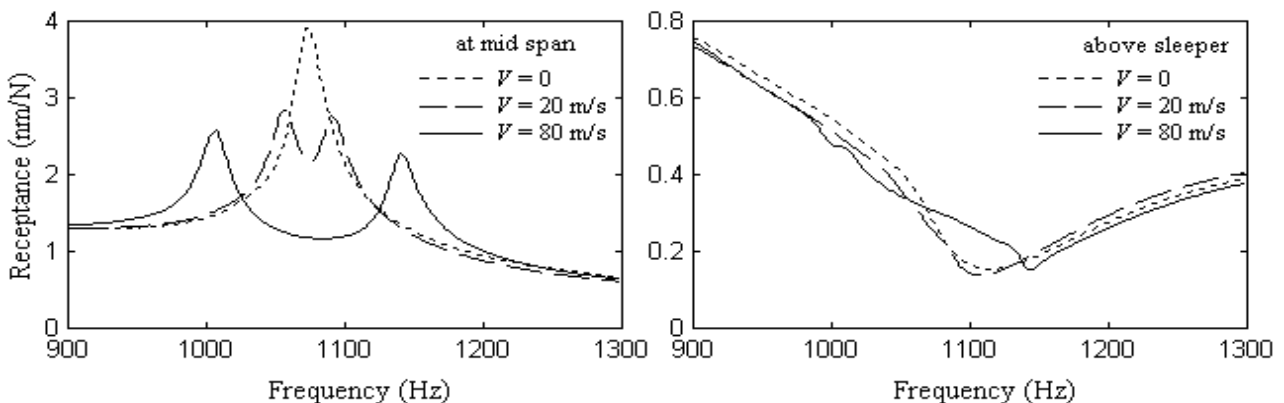


Fig. 3.3.

The rail pad stiffness represents a crucial parameter for the rail dynamic in general, and in particular for the wear of the rolling surface. To illustrate this aspect, the rail pad stiffness of 140 MN/m has been taken into account (elastic rail pad) and the ratio between the rail receptances for the elastic and the reference rail pad has been displayed in Fig. 3.2. The rail receptance is higher at low frequencies due to the elastic rail pad,

especially above sleeper. However, at frequencies above the second resonance (480 Hz), the elastic rail pad has a contrary effect and the rail becomes more rigid, particularly at the mid span. At the pinned-pinned resonance (1074 Hz), it seems that the stiffness of the rail pad has a weak influence on the dynamic behaviour of the rail. At the anti-resonance frequency of the rail above sleeper, the rail receptance is higher when the rail pad is more elastic.

Within the pinned-pinned resonance range, the rail receptance depends on the velocity of unit harmonic load due to the Doppler effect. To concept the idea, one considers the c velocity of the waves that propagate to the right and to the left from the stationary harmonic load. When the harmonic load moves along the rail, the wave that propagates in front of the load has a higher velocity, $c+V$, while the velocity of the wave that propagates behind of the load is lower, $c-V$. Under such circumstances, each wave generates a particular resonance frequency from the resonance condition (the wavelength equals twice the span). This aspect is presented in Fig. 3.3, where the rail receptance above the sleeper and at the mid span for the case of the moving unit harmonic force is shown. As one can see, at the mid span, the peak generated by the stationary harmonic load is replaced by the two peaks produced by the Doppler effect, due to the moving harmonic force. The frequencies of the three peaks are in arithmetic progression, which has the ratio of $V/2d$. For instance, the frequencies of 1 007 and 1 141 Hz correspond to the resonance frequencies due to the Doppler effect at 80 m/s and the span of 0.6 m. The level of the two peaks decreases as the harmonic force speed increases. The rail receptance above sleeper remains practically unchanged.

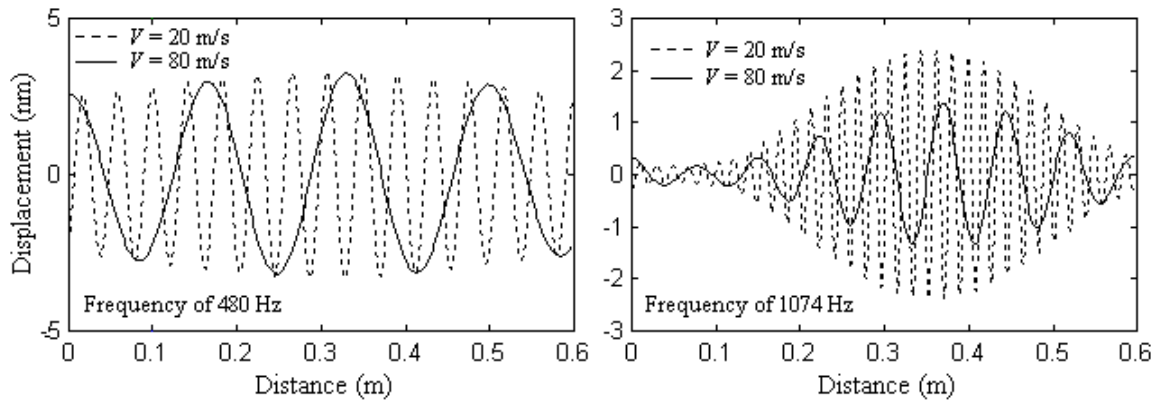


Fig. 3.4.

Figure 3.4 displays the displacement of the rail at the loading point for 20 m/s and 80 m/s and two values of the load frequency, 480 Hz and 1074 Hz. Generally, the motion is modulated due to the periodically support. At 480 Hz, there is no difference between the magnitudes of the loading point displacement for the two velocities and the trajectories of the loading point have the same envelope. On the contrary, at the frequency of 1,074 Hz (pinned-pinned resonance) the force velocity significantly influences the motion of the loading point. The displacement of the loading point is lower for the velocity case of 80 m/s, compared to the one of 20 m/s.

6. CONCLUSIONS

This paper has dealt with the vertical vibration of the ballasted track using a new model for the rail periodic support. The model of the periodic support consists of two three-directional Kelvin-Voigt systems for the rail pad and the ballast, and a mixed Kelvin-Voigt/Maxwell system for the subgrade. Also, the inertia of the sleeper and the ballast block is introduced.

The analysis of the track vibration has been performed in both frequency and time-domain by applying the Green's functions method. The prediction of the rail response corresponds to the results derived from the measurements. The complex influence of the rail pad stiffness on the rail response has been presented for the case of the stationary harmonic load.

For frequencies within the pinned-pinned range, the receptance of the rail has two peaks instead of one due to the Doppler effect. In addition, the time-domain analysis reveals that the rail vibration is the modulated one and the load velocity in the particular pinned-pinned range strongly influences its level. All these features can have an impact on the wheel/rail interaction and the short-pitch formation.

ACKNOWLEDGEMENTS

This work is supported by the NURC (The National University Research Council) under project 1699: *Researches on the wheel/rail parametric vibrations using the track's Green matrix method.*

REFERENCES

1. SHENG, X., THOMPSON, D. J., JONES, C. J. C., XIE, G., IWNICKI, S. D., ALLEN, P., HSU, S. S., *Simulation of roughness initiation and growth on railway rails*, Journal of Sound and Vibration, **293**, pp. 829–829, 2006.
2. REMINGTON, J. P., *Wheel/rail rolling noise: what do we know? What don't we know? Where do we go from here?*, Journal of Sound and Vibration, **120**, pp. 203–226, 1988.
3. GRASSIE, S. L., GREGORY, R. W., HARRISON, D., JOHNSON, K.L. *The dynamic response of railway track to high frequency vertical excitation*, Journal Mechanical Engineering Science, **24**, pp. 77–90, 1982.
4. ZHAI, W. M., WANG, K. Y., LIN, J. H., *Modelling and experiment of railway ballast vibrations*, Journal of Sound and Vibration, **270**, pp. 673–683, 2004.
5. NIELSEN, J. C. O., *High-frequency vertical wheel-rail contact forces-Validation of a prediction model by field testing*, Wear, **265**, pp. 1465–1471, 2008.
6. KNOTHE, K., WU, Y., *Receptance behaviour of railway track and subgrade*, Archive of Applied Mechanics, **68**, pp. 457–470, 1998.
7. MAZILU, Tr., *Propagation of harmonic vertical waves in a rail*, UPB Scientific Bulletin Series D: Mechanical Engineering, **67**, pp. 99–110, 2005.
8. KRZYZYNSKI, T., POPP, K., *On the travelling wave approach for discrete-continuous structures under moving loads*, ZAMM Zeitschrift für Angewandte Mathematik und Mechanik **76** (Suppl.4), pp. 149–152 1996.
9. KRZYZYNSKI, T., *On dynamics of a railway track modelled as a two-dimension periodic structure*, Heavy Vehicle Systems, **6**, pp. 330–344, 1999.
10. SHENG, X., LI, M., JONES, C. J. C., THOMPSON, D. J., *Using the Fourier-series approach to study interactions between moving wheels and a periodically supported rail*, Journal of Sound and Vibration, **303**, pp. 873–894, 2007.
11. NORDBORG, A., *Wheel/rail noise generation due to nonlinear effects and parametric excitation*, Journal of the Acoustical Society of America, **111**, pp. 1772–1781, 2002.
12. MAZILU, Tr., *Green's functions for analysis of dynamic response of wheel/rail to vertical excitation*, Journal of Sound and Vibration, **306**, pp. 31–58, 2007.
13. MAZILU, Tr., *Wheel-rail vibrations* (in Romanian), MatrixRom, 2008.

Received October 20, 2009